

# Char Attrition During the Batch Fluidized Bed Combustion of a Coal

Batchwise fluidized bed combustion of a coal has been carried out to investigate the generation of elutriable carbon fines by attrition of the burning char. Differences between the purely mechanical attrition and the combustion-assisted attrition of the char have been outlined. The time required to "activate" the char surface as regards attrition explains certain features of carbon elutriation curves. Attrition rate constants determined from these curves are compared with those previously found by continuous fluidized combustion of the same coal.

R. CHIRONE, M. D'AMORE,  
L. MASSIMILLA, and  
A. MAZZA

Istituto di Chimica Industriale e Impianti  
Chimici, Università  
Istituto di Ricerche sulla  
Combustione, C.N.R.  
P.le V. Tecchio, 80125  
Napoli, Italy

## SCOPE

The generation of elutriable carbon fines in the fluidized combustion of a coal can be related to coal fragmentation, and to char attrition and combustion. Fragmentation is associated with devolatilization, and results in the break-up of coal into char particles of various sizes. Attrition is due to abrasion of these particles against bed material and the wall of the combustor, and produces fines which are rapidly entrained by the fluidizing gas because of their small size (mostly below  $100\ \mu\text{m}$ ). Both combustion and, to a much lesser degree, attrition itself reduce char particles to sizes at which they are elutriated as unburnt residues from the bed (Beér et al., 1980). Within this framework, char attrition was successfully investigated by means of experiments of continuous fluidized bed combustion (CFBC) of a South African bituminous, nonswelling coal, continuously fed to a 140 mm ID unit (Donsi et al., 1981; Arena et al., 1983). These authors found that under steady-state conditions the attrition contribution to the elutriated carbon rate was proportional to the overall surface of char particles and to the excess of velocity above the minimum fluidizing velocity. A simple relationship of the type  $E_c = k(U - U_o)W_c/\bar{d}$  was shown to hold between four factors: i) the elutriation rate of attrited carbon  $E_c$ , ii) the amount of carbon in the char particles present in the bed, i.e. the bed carbon loading  $W_c$ , iii) the average char particle size  $\bar{d}$ , and iv) the fluidizing velocity excess  $(U - U_o)$ . The attrition rate constant  $k$  of the coal tested remained practically unvaried with changes of coal particle size, gas velocity, bed temperature, coal feed point location, and air excess factor. It was significantly affected only by the size of the sand used as bed inert material.

It might be, however, that CFBC experiments are not the most suitable means for performing a detailed investigation of the attrition behavior of any type of coal. Apart from the impossibility of separating fragmentation fines from attrition fines,

continuous operation means that the measured rates of elutriated carbon integrate the contributions of attrited fines from char particles whose residence times inside the bed cover the entire range from coal devolatilization to almost complete burnout. More appropriate are batch fluidized bed combustion (BFBC) experiments which allow the separation of fragmentation and attrition effects, the time-resolution of attrited fines generation, as well as the study of the influence of combustion on attrition by changing oxygen concentration in the inlet fluidizing gas. This includes the extreme case in which the bed, kept at the combustion temperature by external heating, is fluidized by inert gas so that rates of carbon fines separated from the exit gases are representative of purely mechanical attrition. This work aims at outlining the capabilities of the BFBC technique as resulted from its application to the South African coal already tested in continuous operation. The discussion of the mechanism of generation of carbon fines by attrition revealed by using this technique, and the presentation of a quick method for determining attrition rate constants based on batch combustion data, are within the scope of this work.

It should be noted that a number of works in the literature deal with the batch fluidized bed combustion of carbons and coals (Avedesian and Davidson, 1973; Borghi et al., 1977; Yates and Walker, 1978; Chakraborty and Howard, 1981; Pillai, 1981; Ross and Davidson, 1981; La Nauze and Jung, 1982). These, however, are directed to studying the role of phenomena controlling combustion, without taking into account attrition. Certainly, elutriation of attrited carbon concerns only a small proportion, mostly less than 10%, of carbon injected into the bed, but it is in fact this fraction which is of interest in the design of equipment required to make the fluidized combustion of coals efficient and environmentally acceptable.

## CONCLUSIONS AND SIGNIFICANCE

The proposed BFBC technique is useful in investigating the attrition behavior of a coal under conditions typical of fluidized bed combustion. Time-resolution of elutriated carbon rates is high enough to separate fragmentation from attrition effects and give details on the changes of attrition rates during com-

bustion. In particular, present BFBC results definitely confirm the assumption (Arena et al., 1983) that for the coal in consideration, combustion and attrition of char particles inside the bed occur in parallel. Moreover, they shed light on the enhancing effect that combustion has on attrition. Two types of

attrition have been outlined, depending on whether the bed is fluidized with an inert gas or an oxygen-containing gas: 1) a purely mechanical attrition, characterized by the rapid decay of the elutriation of attrited carbon from an initial high rate typical of angular solids to a lower stationary rate when particles are rounded off (Vaux, 1978), and 2) a combustion-assisted attrition, where detachable asperities are continuously renewed by the irregular movement of the combustion front. Some time is required to fully "activate" the carbon particle surface in respect to combustion-assisted attrition. The rate of this type of attrition is broadly one order of magnitude larger than that of purely mechanical attrition. These phenomena combine with the progressive decrease of the surface of the burning particle in determining the shape of attrition curves, with an initial peak and a relative maximum located somewhere afterward.

Working out BFBC data gives attrition rate constants  $k$  in fair agreement with those previously found, as an average, for the same coal from CFBC results (Donsi et al., 1981; Arena et al.,

1983). In particular, the relationship  $E_c = k(U - U_o)w_c/\bar{d}$  holding for these results can be extended to BFBC data in the form  $e_c = k(U - U_o)w_c/\bar{d}$ , where  $e_c$ ,  $w_c$  and  $\bar{d}$  are, respectively, the instantaneous elutriated carbon rate, bed carbon loading, and char particle average size. A rapid procedure for determining  $k$  is based on the regression straight line correlating data points of these variables collected at different times in a single BFBC run. This further confirms the usefulness of BFBC experiments as regards testing char attrition in fluidized combustion of coals. These experiments can be carried out rapidly and with small-scale apparatus, and are therefore suitable for developing into a standard technique to compare different coals and evaluate attrition rate constants to be embodied in model calculations. A limit in scaling down the testing apparatus derives from the size of coal and bed material being considered. For given sizes, the diameter of the combustor should be sufficiently large to ensure thorough mixing of coal inside the fluidized bed solids.

## EXPERIMENTAL

### Materials

The coal used in this work is the South African bituminous, nonswelling coal whose attrition behavior has already been studied by means of CFBC experiments by Donsi et al. (1981) and Arena et al. (1983). The properties of the coal were reported in detail by the latter authors. In particular, coal content of fixed carbon, volatile matter, and ash is about 60, 25, and 15%, respectively. Alternatively, char of the same coal, separately prepared in a fluidized bed at the temperature at which the attrition experiment is performed, has been used for comparison in some runs. Particle sizes of batches of coal and char tested are given in Table 1. Distributions of particle size of char formed inside the bed by fragmentation when using the various batches of coal are also given in this table, together with devolatilization

times. Batches of char did not show further fragmentation when injected into the bed. 0.4–0.3 mm sand was used as bed solids. Unexpanded bed height was about 100 mm.

### Experimental Apparatus and Technique

The batch fluidized bed combustion (BFBC) technique adopted for determining the rate of generation of carbon fines by fragmentation and attrition is based on the measurement of the rate of carbon fines elutriated from the bed and collected downstream of the combustor at given times after injecting a batch of coal (or char) into the bed. Attrition fines are generated throughout the combustion time of the batch, from injection to burnout; fragmentation fines are generated only during the small fraction of time from injection to the end of devolatilization, and only when coal is used. An apparatus consisting of a 40 mm ID and 1 m high combustor with a two-exit head was specifically developed for these experiments. Carbon elutriation rates were supplemented with particle size distributions and carbon content of the char present in the bed. These were obtained in parallel experiments with another combustor also of 40 mm ID but equipped with a basket made of a 0.6 mm mesh to allow collection of char from the bed according to the Andrei (1979) technique. The two-exit head combustor and the basket-equipped combustor are presented in Figures 1-I and 1-II, respectively. Details about design and operation of these combustors are given elsewhere (Chirone et al., 1982). Only their main features are briefly described in the following.

The two-exit head combustor is operated by means of the three-way ball valve (11) in Figure 1-I. The proper position of this valve allows the collection of fines in the filter connected to one of the exits during the substitution of the other filter. The connection is alternatively made with the two exits. Using several filters in sequence, carbon emission within the combustion time after coal or char has been charged into the bed through the hopper (5) could be conveniently time-resolved. To keep oxidizing conditions substantially uniform during the combustion time, batches of only 3.4 g of coal (or 2.5 g of char) were used in each run, corresponding to a constant amount  $w_{cf}$  of 2.0 g of fixed carbon initially charged into the bed. For given experimental conditions, operation was repeated with various batches of coal or char of the same size to allow the accumulation in each filter of an amount of fines large enough to make weighing and chemical analysis reliable. Knowing the amount of carbon collected in a given time interval of the combustion cycle and the number of repeated cycles, an instantaneous carbon elutriation rate  $e_c$  could be determined and assigned at the mean point of the time interval in consideration. To minimize postcombustion of carbon fines, the temperature in the freeboard was kept as low as possible by limiting the thermal insulation of the combustor to a height equal to bed height. Neglecting postcombustion inside the bed and in the freeboard implies assuming that the rates of generation of carbon fines in the bed were equal to the rates of collection of carbon fines in the filters. At bed temperature of 850°C, the latter was up to 30% smaller, depending on the size of fines and oxygen concentration in inlet gas. This was shown by the results of a separate investigation carried out by measuring the degree of combustion of carbon fines continuously fed to the bed of the combustor shown in Figure 1-I. For given experimental conditions, burnout time  $t_{bo}$  was determined as the time at which CO<sub>2</sub> concentration

TABLE 1. EXPERIMENTAL CONDITIONS

| Operative Variables of the Combustors                    |   |                              |                                      |                            |
|--|---|------------------------------|--------------------------------------|----------------------------|
| Bed Temperature, °C                                      | 750,850,950   |                              |                                      |                            |
| Fluidizing Velocity, cm s <sup>-1</sup>                  | 50 ( <i>d</i> * ≈ 120 μm), 80 ( <i>d</i> * = 179 μm),<br>110 ( <i>d</i> * = 200 μm) |                              |                                      |                            |
| O <sub>2</sub> % in Inlet and<br>Outlet Gas†             | 0, 0.75(0.58), 1.4(1.1), 2.9(2.2), 4.5(3.5),<br>21(16.7)                            |                              |                                      |                            |
| Size Distribution of the Batches of Coal and Char Tested |   |                              |                                      |                            |
| Coal Feed  |   |                              |                                      |                            |
| Feed Size<br><i>d<sub>t</sub></i> , mm                   | Devolatilization<br><i>t<sub>dev</sub></i> , s                                      | Char from Coal Fragmentation |                                      |                            |
| <i>d<sub>t</sub></i> , mm                                | <i>t<sub>dev</sub></i> , s  | <i>d<sub>t</sub></i> , mm    | <i>X<sub>d<sub>t</sub></sub></i> , % | <i>d̄<sub>t</sub></i> , mm |
| 4.76–4.00  | 20  | 4.76–4.00                    | 92.26                                | 4.25                       |
|  |   | 4.00–3.00                    | 6.80                                 |                            |
|  |   | 3.00–2.00                    | 0.54                                 |                            |
|  |   | 2.00–0.60                    | 0.40                                 |                            |
| 6.35–4.76  | 25  | 6.35–4.76                    | 85.64                                | 4.84                       |
|  |   | 4.76–4.00                    | 5.54                                 |                            |
|  |   | 4.00–3.00                    | 4.23                                 |                            |
|  |   | 3.00–2.00                    | 2.11                                 |                            |
| 9.00–6.35  | 30  | 2.00–0.60                    | 2.48                                 |                            |
|  |   | 9.00–6.35                    | 54.02                                | 5.36                       |
|  |   | 6.35–4.76                    | 28.62                                |                            |
|  |   | 4.76–4.00                    | 5.21                                 |                            |
|  |   | 4.00–3.00                    | 6.51                                 |                            |
|  |   | 3.00–2.00                    | 2.45                                 |                            |
|  |   | 2.00–0.60                    | 3.19                                 |                            |
| Char Feed  |   |                              |                                      |                            |
| <i>d<sub>t</sub></i> , mm                                |   |                              |                                      | <i>d̄<sub>t</sub></i> , mm |
| 6.35–4.76  |   |                              |                                      | 5.56                       |

† O<sub>2</sub>% in outlet gas (in parentheses) is the minimum oxygen concentration read at the analyzer during the combustion of the batch of coal.

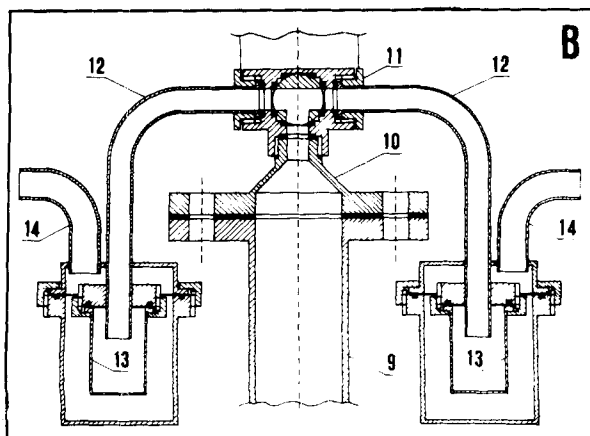
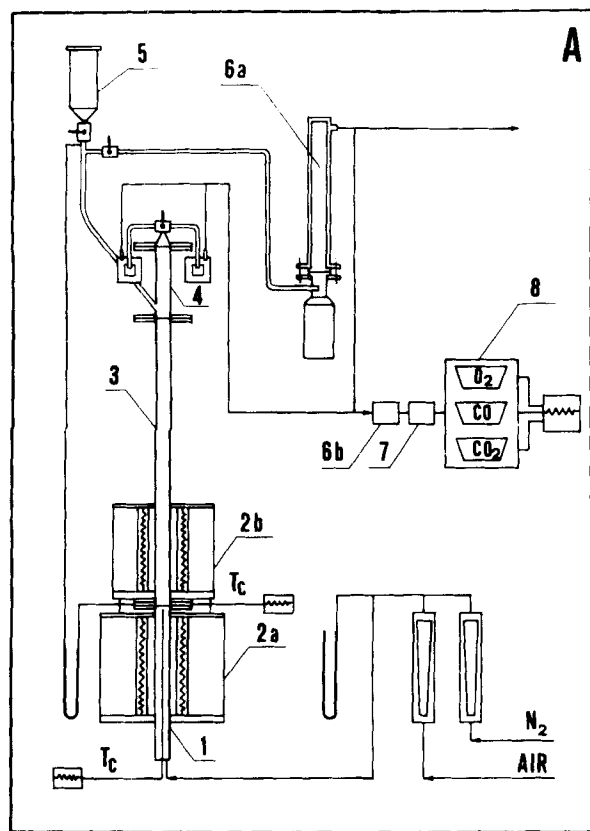


Figure 1-I. Fluidized bed two-exit head combustor used in attrition experiments. A. The apparatus: (1) air preheater; (2a) (2b) electric furnaces; (3) fluidization column; (4) two-exit head; (5) hopper; (6a) (6b) flue gas filters; (7) pump; (8) O<sub>2</sub>, CO, CO<sub>2</sub> analyzers. B. Two-exit head, front view; (9) brass tube; (10) cone-shaped duct; (11) three-way ball valve; (12) pipes to filters; (13) brass filters; (14) pipes to analyzers.

dropped to zero in exit gases. From the known  $w_{c1}$  and the amount of carbon which had left the combustor at a given time as CO<sub>2</sub> and CO, the bed carbon loading  $w_c$ , i.e., the amount of carbon still present inside the bed at that time, could be calculated.

The basket-equipped combustor is operated by means of the basket holder (1) in Figure 1-II. It is moved up and down along the guide (2) and pivoted around the axis (8) in order to locate the basket in the bed, pull it out, and discharge collected solids. Batches of coal or char, again 3.4 g or 2.5 g, respectively, are injected in the bed and left there for a given time, until combustion is interrupted by switching fluidizing gas from the oxygen-nitrogen mixture to nitrogen. Char present in the bed at that time is collected with the basket. Nitrogen issuing from a channel between the basket holder and an outer tubing quenches the char and prevents its further burning in the atmosphere. Weighing, sieving, and analyzing the collected material for carbon content allows evaluation at any time between coal or char injection and burnout of: 1) the mass fraction  $C$  of carbon in the char, 2) the bed carbon loading  $w_c$ , i.e. the amount of carbon in the char particles

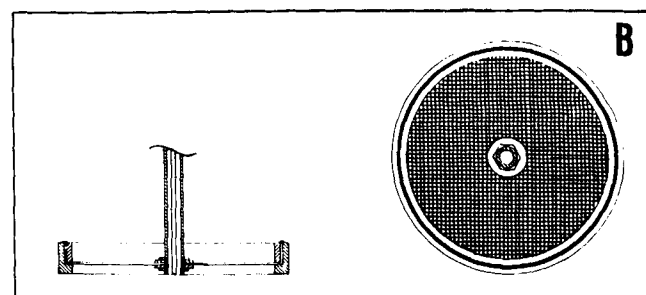
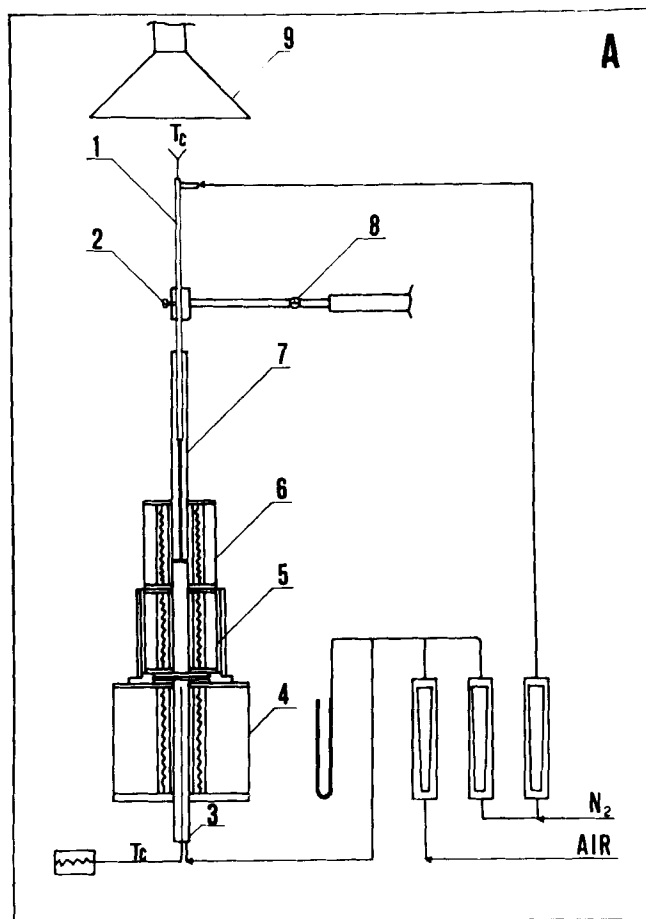


Figure 1-II. Fluidized bed combustor used in fragmentation experiments. A. The apparatus: (1) basket holder; (2) basket holder guide; (3) air preheater; (4) preheater electric furnace; (5) (6) fluidization column electric furnaces; (7) quartz tube; (8) spherical pivot for basket holder; (9) stack. B. Basket, front and top views.

found in the bed, and 3) the fraction  $X_d$  of bed carbon contained in the char particle of size  $d$  and the surface based average bed char particle sizes  $\bar{d} = 1/\sum X_d/d$ . In particular, measurements on material collected at the end of devolatilization time of each batch of coal gave the initial mass fraction  $C_i$  of carbon and the initial distribution and average particle size  $\bar{d}_i$  of the fragmented coal reported in Table 1. The lower limit of this distribution reflects the fact that only fragmented char coarser than 0.6 mm, i.e. coarser than the mesh opening, could be collected with the basket. The amount of finer fragments, however, accounted for less than 0.5% of  $w_{c1}$  as proved by burning the amount of carbon left in the bed. Note that the initial size distribution of fragmented coal was not affected by whether nitrogen or an oxygen-nitrogen mixture was used as fluidizing gas. Values of  $w_c$  determined with the basket technique and from gas analysis using the combustor of Figure 1-I were equal to each other within an error of 3%.

Oxygen concentrations in inlet gas, fluidizing velocities, and bed temperatures at which BFBC experiments were carried out are listed in Table 1. Differences between oxygen concentration in inlet and outlet gas changed during the combustion cycle from a maximum occurring soon after injecting coal or char into the bed to zero at  $t = t_{bo}$ . For a given oxygen concentration in inlet gas, typical values of the minimum oxygen concentration in outlet gas are also reported in Table 1.

TABLE 2. CHARACTERISTIC VALUES OF ATTRITION CURVES

| $d_i$<br>mm | $U$<br>$\text{cm s}^{-1}$ | $T$<br>$^{\circ}\text{C}$ | $(\text{O}_2)$ in<br>% | Coal Feed   |                 | $e_{cl}$<br>$10^{-3}$ g | $e'_c$<br>$\text{min}^{-1}$ | $w'_c$<br>g | $\frac{w_{cl}-w_c}{w_{cl}}$ | $1-\eta$ |
|-------------|---------------------------|---------------------------|------------------------|-------------|-----------------|-------------------------|-----------------------------|-------------|-----------------------------|----------|
|             |                           |                           |                        | $t'$<br>min | $t_{bo}$<br>min |                         |                             |             |                             |          |
| 4.76-4.00   | 80                        | 850                       | 4.5                    | 4.5         | 46              | 2.2                     | 2.9                         | 1.54        | 0.25                        | 0.029    |
| 6.35-4.76   | 50                        | 850                       | 4.5                    | 10.0        | 68              | 3.7                     | 1.2                         | 1.38        | 0.32                        | 0.021    |
| 6.35-4.76   | 80                        | 750                       | 21                     | 2.2         | 18              | 6.6                     | 4.7                         | 1.35        | 0.34                        | 0.010    |
| 6.35-4.76   | 80                        | 750                       | 4.5                    | 7.2         | 68              | 13.4                    | 3.5                         | 1.44        | 0.29                        | 0.063    |
| 6.35-4.76   | 80                        | 850                       | 21                     | —           | 15              | 6.7                     | —                           | —           | —                           | 0.010    |
| 6.35-4.76   | 80                        | 850                       | 4.5                    | 6.8         | 56              | 3.8                     | 2.9                         | 1.44        | 0.29                        | 0.037    |
| 6.35-4.76   | 80                        | 850                       | 2.9                    | 10.8        | 84              | 5.6                     | 2.7                         | 1.54        | 0.25                        | 0.056    |
| 6.35-4.76   | 80                        | 850                       | 1.4                    | 18.3        | 160             | 7.6                     | 1.6                         | 1.60        | 0.22                        | 0.061    |
| 6.35-4.76   | 80                        | 850                       | 0.75                   | 32.8        | 360             | 9.0                     | 1.4                         | 1.53        | 0.25                        | 0.108    |
| 6.35-4.76   | 80                        | 850                       | 0                      | —           | —               | 3.4                     | —                           | —           | —                           | 1        |
| 6.35-4.76   | 80                        | 950                       | 4.5                    | 2.5         | 54              | 4.0                     | 1.3                         | 1.80        | 0.12                        | 0.019    |
| 6.35-4.76   | 110                       | 850                       | 4.5                    | 5.9         | 52              | 12.2                    | 4.6                         | 1.46        | 0.29                        | 0.054    |
| 9.00-6.35   | 80                        | 850                       | 4.5                    | 5.7         | 68              | 3.0                     | 2.8                         | 1.66        | 0.19                        | 0.043    |
| Char Feed   |                           |                           |                        |             |                 |                         |                             |             |                             |          |
| 6.35-4.76   | 80                        | 850                       | 21                     | 2.5         | 18              | 1.8                     | 2.2                         | 1.28        | 0.37                        | 0.007    |
| 6.35-4.76   | 80                        | 850                       | 4.5                    | 6.8         | 60              | 2.3                     | 2.9                         | 1.52        | 0.25                        | 0.037    |
| 6.35-4.76   | 80                        | 850                       | 1.4                    | 20.2        | 160             | 4.9                     | 1.5                         | 1.50        | 0.27                        | 0.058    |
| 6.35-4.76   | 80                        | 850                       | 0                      | —           | —               | 2.9                     | —                           | —           | —                           | 1        |

Unfortunately, investigation with bed sands of size coarser than 0.4 mm was impossible because these sands helped produce pistonlike fluidizations in the 40 mm ID combustor. This, in turn, caused severe segregation of char on the top of the bed. Moreover, it was impractical to extend the experimental range of fluidizing gas velocities. Due to the limited freeboard height, the proportion of elutriated char particles coarser than  $d^*$ , the size of particles whose free-fall velocity is equal to the gas velocity at the combustor exit, significantly increased at gas velocities above  $110 \text{ cm s}^{-1}$ . This made the evaluation of rates of generation of attrition fines from measured rates of carbon collected at the filters unreliable. Values of  $d^*$  at the three levels of gas velocities tested are given in Table 1. Both these experimental limitations might be overcome by means of combustors of larger size than those used, but at the expense of some complication in experimental installations and procedures.

The granulometric analysis of carbon fines collected in the filters of the combustor of Figure 1-I was made for one of the experimental conditions tested. The photographic technique used permitted distinguishing between ash and char of particle size as low as  $3 \mu\text{m}$ .

## EXPERIMENTAL RESULTS

The generation of elutriable carbon fines, i.e. of carbon particles finer than  $d^*$ , is associated with fragmentation, which in turn depends on devolatilization, and with attrition. Devolatilization and fragmentation are not expected to occur when injecting char directly into the bed. Therefore, the differences in the amounts of carbon collected at the filters of the combustor of Figure 1-I throughout the devolatilization time when charging coal and char, all other conditions remaining the same, account for the contribution of fragmentation fines. These differences are of about  $10^{-3}$

g, i.e. less than 0.1% of fixed carbon  $w_{cl}$  charged into the bed. This confirms the negligible tendency of the coal tested to produce fragmentation fines during devolatilization.

Whatever the experimental conditions, carbon dioxide and carbon fines are simultaneously found throughout the time interval between injection and burnout at the combustor exit. This is in agreement with the model suggested by Arena et al. (1983) which considers attrition as a side process of fluidized bed combustion. The yield in attrited carbon, however, is small, being at most about 10% of  $w_{cl}$  at low inlet oxygen concentration in fluidizing gas.

Following these general conclusions, average particle sizes and carbon contents of bed char obtained by means of the basket-equipped combustor and instantaneous elutriation rates of attrited carbon, correspondingly obtained by means of the two-exit head combustor, will be presented and discussed separately. The whole data will subsequently be combined in testing attrition rate equations.

## Char Shrinkage Curves

The progress of shrinkage of char particles is expressed in terms of the ratio  $\bar{d}/\bar{d}_i$  of the actual average char size  $\bar{d}$  to the initial average size  $\bar{d}_i$  as a function of the fractional conversion  $\xi = (w_{cl} - w_c)/w_{cl}$  of fixed carbon injected into the bed (Figure 2) and of the ratio  $t/t_{bo}$  of the time  $t$  after injection to the burn-out time  $t_{bo}$  (Figure 3). Average sizes  $\bar{d}_i$  are given in Table 1, burnout times  $t_{bo}$  in Table 2. Then, knowing  $w_{cl}$ ,  $\bar{d}_i$  and  $t_{bo}$ , values of  $w_c$  and  $\bar{d}$  to be used in attrition rate equations can be obtained from Figures 2 and 3 at any time for each experimental condition tested. The

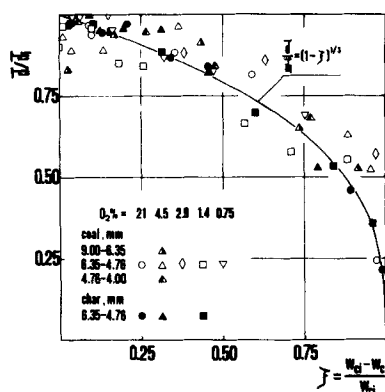


Figure 2. Char particle shrinkage as a function of fractional conversion of carbon.  $U = 80 \text{ cm s}^{-1}$ ;  $T = 850^{\circ}\text{C}$ .

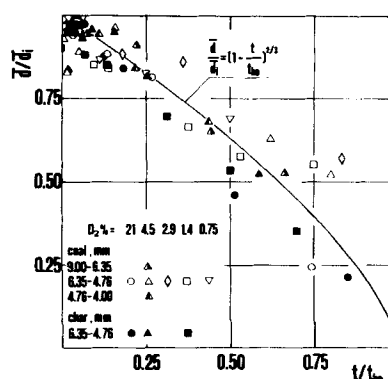


Figure 3. Char particle shrinkage as a function of time.  $U = 80 \text{ cm s}^{-1}$ ;  $T = 850^{\circ}\text{C}$ .

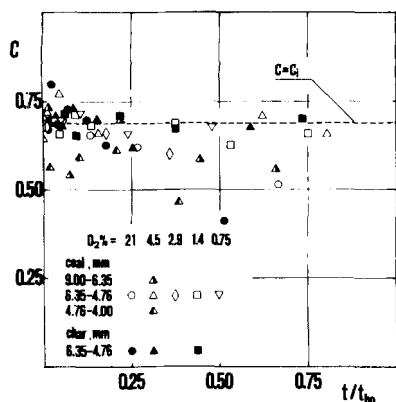


Figure 4. Mass fraction of carbon in the char as a function of time.  
 $U = 80 \text{ cm s}^{-1}$ ;  $T = 850^\circ\text{C}$ .

carbon content  $C$  of the char particles at time  $t$  after injection is reported as a function of  $t/t_{bo}$  in Figure 4.

Data in Figures 2, 3, and 4 are respectively compared with the following expressions

$$\frac{\bar{d}}{d_i} = (1 - \xi)^{1/3} \quad (1)$$

$$\frac{\bar{d}}{d_i} = \left(1 - \frac{t}{t_{bo}}\right)^{2/3} \quad (2)$$

$$C = C_i \quad (3)$$

derived from a carbon balance around the particle, Eqs. 1 and 3, and between the particle and surrounding gas, Eq. 2. In this latter equation  $C_i$  is the average initial carbon content of devolatilized coal. Equations 1 and 3 imply that conversion takes place at a constant mass fraction of carbon in the char, i.e. that the shrinking particle model applies (Levenspiel, 1972; La Nauze and Jung, 1982; Jung and La Nauze, 1983). Equation 2 assumes that, considering the coarse size of particles over a large fraction of the time interval from injection to burnout, the rate-controlling step is oxygen diffusion to carbon (Levenspiel, 1972). Char shrinkages and carbon contents are approximately represented by these equations for the majority of experimental conditions tested. Note, however, that the validity of the shrinking particle model described by Eqs. 1 and 3 refers to the behavior of the particle in its entirety. Actually, oxygen penetrates somewhat inside the particle, depending on the size of the pore, particle temperature, and oxygen concentration for reaction kinetics order different from one. On the average, such penetration is likely to be small, but it is in fact the mechanical structure of the cortical region of the particle which affects attrition. In any case, consistent with the shrinking particle model, the instantaneous removal of ash from this region has been assumed.

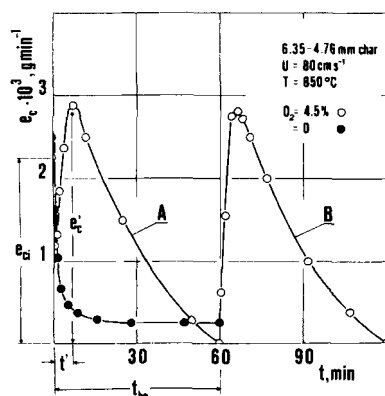


Figure 5. Carbon elutriation curves: ● purely mechanical attrition; ○ combustion-assisted attrition.

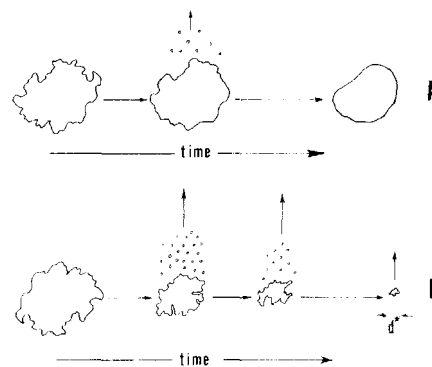


Figure 6. Model representation: A, purely mechanical attrition; B, combustion-assisted attrition.

## Attrition Curves

**Influence of combustion on attrition.** Curves of instantaneous elutriation rates in Figure 5 describe some features of char attrition under inert and oxidizing conditions. Without oxygen, the  $e_c$  vs.  $t$  curve (black circles) is that typical of purely mechanical attrition of angular solids in fluidized beds (Vaux, 1978). The peak value  $e_{ci}$  at  $t = 0$  is the initial attrition related to the detachment of asperities from the char surface. Rounding off surface irregularities results in the decay of the elutriation rate to a low value of  $e_c$  after about 30 min of operation. Further decrease of  $e_c$  associated with the reduction of exposed particle surface is very slow, due to the long time required to significantly change particle size only by attrition. A peak value  $e_{ci}$  is also found with 4.5%  $O_2$  in fluidizing gas (open circles of curve A), but in this case, after a temporary decay  $e_c$  increases rapidly again. It reaches a maximum  $e_c$  at  $t = t'$  and eventually declines slowly to reach zero at 60 min, which is the burnout time  $t_{bo}$  of char under the conditions tested. The maximum  $e_{ci}'$  recently found in the attrition curves of a number of other coals (Massimilla et al., 1983), may derive from the opposite effects of two phenomena developing during the combustion of the char particle: 1) the uneven progress of the combustion front, which results in the generation and growing of detachable asperities, and 2) the reduction of the surface of the burning particle, which reduces the total number of asperities available for detachment. The "activation" of char surface in respect to attrition induced by combustion was ascertained by means of an experiment whose results are also shown in Figure 5 (open circles of curve B). At  $t = 60$  min, when the low value of  $e_c$  under inert conditions had been reached, fluidizing gas was suddenly switched from nitrogen to an oxygen-nitrogen mixture with 4.5%  $O_2$ . Combustion was responsible for the rapid increase of  $e_c$  in this case. But apart from the initial attrition which had been suppressed in the curve B by the pretreatment of the char, the  $e_c$  vs.  $t$ , curves A and B are exactly the same.

Note that the rate of combustion-assisted attrition is much larger than that of purely mechanical attrition. With reference to the left side of Figure 5,  $e_c$  averaged over the 60 min between injection and burnout is in the first case (open circles) about five times greater than in the second case (black circles). A conceptual representation of purely mechanical and combustion-assisted attrition is shown in Figure 6.

**Attrition curve shape and characteristic points.** Attrition curves from experiments at  $850^\circ\text{C}$  and fluidizing velocity of  $80 \text{ cm s}^{-1}$  with 6.35–4.76 mm char and coal are respectively reported in Figures 7 and 8. Changing from char to coal does not result in differences in the elutriation curve except as regards the effects of coal fragmentation fines on the initial peak value  $e_{ci}$  at  $t = 0$ . Particle size distributions of carbon fines collected at various times for the run with coal feed and 4.5%  $O_2$  in inlet gas are presented in Figure 9. The distributions are expressed on a numerical basis due to the difficulties of assigning a carbon density to relatively coarse char fines ( $>100 \mu\text{m}$ ) whose micrographs present substantial intraparticle voids. These coarser particles, collected in larger

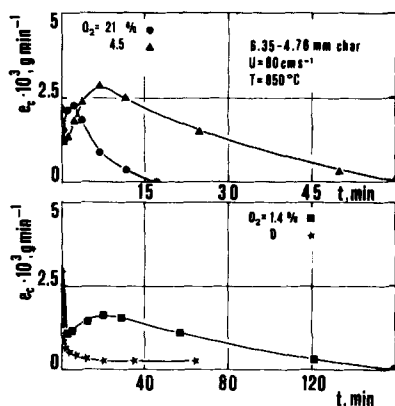


Figure 7. Attrition curves for char feed: influence of oxygen concentration in inlet gas.

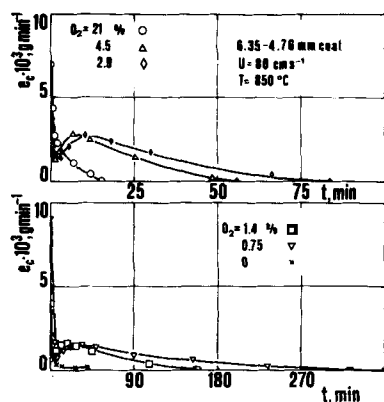


Figure 8. Attrition curves for coal feed: influence of oxygen concentration in inlet gas.

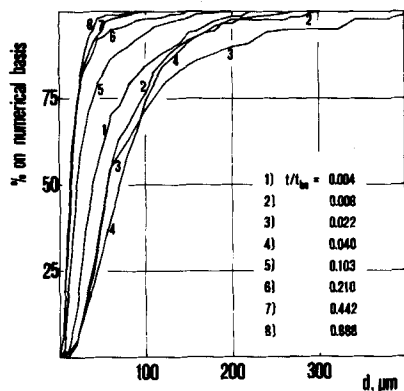


Figure 9. Cumulative particle size distribution of carbon fines collected at filters during time from injection to burnout.

6.35-4.76 mm coal  
 $U = 80 \text{ cm s}^{-1}$   
 $T = 850^\circ\text{C}$   
 $\% \text{O}_2 \text{ in inlet gas} = 4.5$   
 $t_{bo} = 56 \text{ min}$

proportion in the first minutes after injection, are probably the fragmentation fines or their unburnt residues.

Attrition curves similar to those of Figure 8 are obtained feeding 4.76-4.00 and 9.00-6.35 mm coal, Figure 10. The presence of the maximum  $e_c$  depends on the severity of oxidation conditions as determined by both bed temperature and oxygen concentration in inlet gas. As shown in Figure 11, at  $750^\circ\text{C}$   $e_c$  occurs at 2.2 min for 21%  $\text{O}_2$  in fluidizing gas. At  $850^\circ\text{C}$  and the same oxygen concentration this maximum disappears. On the other hand, the values of  $e_c$  and the shape itself of the attrition curve at  $950^\circ\text{C}$  and 4.5%  $\text{O}_2$  might have been influenced by significant postcombustion of attrited carbon under these conditions.

Table 2 gives the characteristic values of attrition curves for all

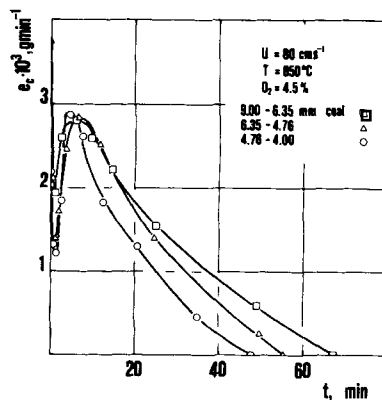


Figure 10. Attrition curves for coal feed: influence of feed size.

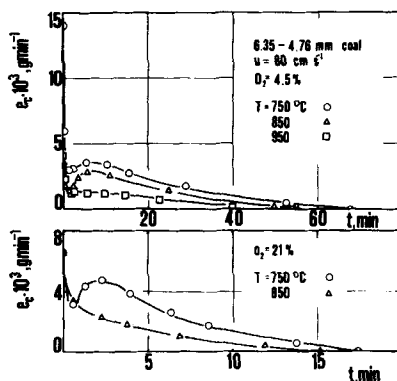


Figure 11. Attrition curves for coal feed: influence of bed temperature at two levels of oxygen concentration in inlet gas.

the experimental conditions tested, namely:  $e_{c,t}$ ,  $e'_c$ , the time  $t'$  at which  $e'_c$  appears, the carbon loading  $w'_c$  at  $t'$ , and the fraction  $(w_{c,t} - w'_c)/w_{c,t}$  burnt at  $t'$ . The fraction of unburnt carbon elutriated as attrited fines is related to carbon combustion efficiency  $\eta$  by the relationship:

$$1 - \eta = \int_0^{t_{bo}} \frac{e_c}{w_{c,t}} dt \quad (4)$$

The losses of combustion efficiency  $(1 - \eta)$  due to char attrition are also reported in the table.

It is worth noting that for given coal feed size both  $t_{bo}$  and  $(1 - \eta)$  increase as oxygen concentration in inlet gas and bed temperature decrease. This is in accordance with the fact that, as observed by D'Amore et al. (1980), attrition being a side phenomenon in respect to combustion, the longer the burnout time, the higher the loss of attrited carbon entrained in exit gas. ( $\text{O}_2$ )<sub>in</sub> less than 0.75% would result in  $(1 - \eta)$  larger than 0.108, being as a limit case  $1 - \eta = 1$  for 0%  $\text{O}_2$ . Results of present work suggest, however, that exposure time of the char particle in the bed is not the only variable determining the overall carbon elutriation by attrition. The amount of material effectively detached per collision between the char particle and bed solids might also be important. For instance, the loss of combustion efficiency due to attrited carbon in experiments with 0.75%  $\text{O}_2$  over the long exposure time of 360 min (Table 2) though high could have been somewhat limited by the low concentration of surface asperities. It is in fact possible that the conditions of the char surface in such a run were similar to those described in Figure 6 for purely mechanical attrition.

## ATTRITION RATE

### Evaluation of Rate Equation Constants

The attrition model is based on the assumption that the instantaneous rate of carbon fines detached from an individual char

particle is proportional to the exposed surface as well as to the excess of gas velocity  $U$  above the minimum for fluidization  $U_o$  (Donsi et al., 1981). A similar assumption as regards the influence of fluidizing velocity was made by Merrick and Highley (1974) in their study on attrition of coal ashes in a fluidized bed combustor. With the further hypothesis that the shrinking particle model applies, the rate of loss of carbon by attrition experienced by a spherical char particle of diameter  $d$  is

$$\left(-\rho_c \frac{\pi}{6} \frac{dd^3}{dt}\right)_a = k'_a (U - U_o) \pi d^2 \quad (5)$$

where  $\rho_c$  is the carbon density of the char particle, i.e. the mass of carbon per unit particle volume, and  $k'_a$  is the attrition rate constant of the char. From Eq. 5 the attrition contribution to the shrinkage rate of the particle is obtained

$$\left(-\frac{dd}{dt}\right)_a = k_a (U - U_o) \quad (6)$$

in which

$$k_a = \frac{2k'_a}{\rho_c} \quad (7)$$

Considering both diffusional and chemical kinetics control, and assuming complete mixing of gas in the particulate phase, first-order reaction, and conversion of carbon to  $\text{CO}_2$ , the combustion contribution to the shrinkage of the char particle is

$$\left(-\frac{dd}{dt}\right)_c = \frac{c_p}{\frac{d\rho_c}{2M_c Sh D_g} + \frac{\rho_c}{2M_c k_s}} \quad (8)$$

where  $c_p$  is the oxygen concentration in the particulate phase,  $\rho_c/M_c$  is the carbon molar density of the char particle,  $Sh$  is the particle Sherwood number,  $D_g$  is the oxygen diffusivity, and  $k_s$  is the reaction rate constant at the particle effective temperature (Donsi et al., 1979). The overall shrinkage rate is

$$-\frac{dd}{dt} = \left(-\frac{dd}{dt}\right)_c + \left(-\frac{dd}{dt}\right)_a \quad (9)$$

which enters in the population balance equation of char particles in modeling a continuous fluidized bed combustor (Kunii and Levenspiel, 1969).

Taking into account Eq. 5, the elutriation rate  $E_c$  of attrited carbon from a continuous combustor is obtained by integrating the attrition contribution from all the char particles to be found in the bed at different stages from coal devolatilization to almost burnout. If  $k'_a$  is the same for all the particles, i.e. if  $k'_a$  remains unchanged as each particle shrinks from its original size  $d_i$  to the elutriable size  $d^*$ , it is

$$E_c = k'_a \pi (U - U_o) \int_{d^*}^{d_i} d^2 P(d) dd \quad (10)$$

$P(d)$  being the bed char particle size distribution on a numerical basis. On the other hand, the overall bed char exposed surface  $\pi \int_{d^*}^{d_i} d^2 P(d) dd$  can be expressed as a function of bed carbon loading  $W_c$  and surface-based average particle size  $\bar{d}$ . It is in fact

$$\bar{d} = \frac{1}{\int_{d^*}^{d_i} \frac{d^4 P_w(d) dd}{d}} \quad (11)$$

where the size distribution on weight basis  $P_w(d)$  is related to  $P(d)$  and  $W_c$  by the relationship

$$P_w(d) = \frac{\frac{\pi}{6} \rho_c d^3 P(d)}{W_c} \quad (12)$$

Substituting between Eqs. 10, 11, and 12, and putting

$$k = \frac{6k'_a}{\rho_c} \quad (13)$$

gives

$$k = \frac{E_c}{(U - U_o) \frac{W_c}{\bar{d}}} \quad (14)$$

Attrition rate constants were determined by Donsi et al. (1981) and Arena et al. (1983) by entering into this relationship with the values of the attrited carbon rates  $E_c$ , carbon loading  $W_c$ , and average char particle size  $\bar{d}$  from CFBC experiments, and determining  $k$  as the slope of a regression straightline in the diagram  $E_c$  vs.  $(U - U_o) W_c/\bar{d}$ . The value of  $k$  was invariable to changes in most operating conditions. Significant variations were only found when changing bed solids size. In particular, in view of further comparison with results from BFBC experiments, the value of  $k$  relative to all the runs with 0.2–0.4 mm sand for the entire experimental range of oxygen concentration in outlet gas ( $0.5 < (\text{O}_2\%)_{\text{out}} < 7$ ) is given in Table 3 together with values of  $k$  determined for sets of runs characterized by narrower ranges of  $(\text{O}_2\%)_{\text{out}}$ .

Although the  $e_c$  vs.  $t$  curves from BFBC experiments fully describe the attrition behavior of the char in consideration, their use in predicting carbon loss by attrition from a continuous combustor is not straightforward even under the simplifying assumptions that coal feed is narrow size and that fragmentation is negligible. In this case, if  $N$  is the number of coal particles used in the BFBC experiments, the instantaneous rate of attrited carbon lost by each char particle  $(-\rho_c \pi/6 dd^3/dt)_a$  is  $e_c(t)/N$ , which can be converted into  $e_c(d)/N$  due to the biunivocal relationship between  $t$  and  $d$  given by the char shrinkage curve. This leads to the equation for the rate of attrited carbon loss from the continuous combustor:

$$E_c = \int_{d^*}^{d_i} \frac{e_c(d)}{N} P(d) dd \quad (15)$$

Such an equation is the counterpart of Eq. 10 used in working out results from CFBC experiments, but is difficult to handle because of the lack of knowledge of the size distribution  $P(d)$  of the char particles to be found in the bed. On the other hand,  $P(d)$  cannot be calculated separately because it is related within the char particle population balance equation to combustion and attrition itself through the shrinkage rates respectively given by Eqs. 8 and 6. These difficulties and in particular those arising when extending this procedure to multisize feed and fragmentable coal, discourage the direct use of attrition curves in design application.

Alternatively, char shrinkage and attrition curves from BFBC experiments can be worked out together to give attrition rate constants defined, in similarity with Eq. 14, as  $e_c/[(U - U_o)w_c/\bar{d}]$ . Their averages over  $t_{bo}$

$$k = \frac{\int_0^{t_{bo}} \frac{e_c}{(U - U_o)w_c/\bar{d}} dt}{t_{bo}} \quad (16)$$

are given in Table 3 for the various BFBC runs. Inspection of data indicates that  $e_c/[(U - U_o)w_c/\bar{d}]$  in Eq. 16 becomes practically constant at  $t \geq t'$ , so that an approximated value of  $k$  can be expressed within the time interval  $(t_{bo} - t')$  by means of the relationship

$$k = \frac{e_c}{(U - U_o) \frac{w_c}{\bar{d}}} \quad (17)$$

The attrition rate constant is determined in this case as the slope of regression straight lines in the diagram  $e_c$  vs.  $(U - U_o) w_c/\bar{d}$  as shown in Figures 12 and 13 for experiments with char and coal respectively. Data points in these figures are obtained by directly using the experimental values of  $e_c$  in the attrition curves, whereas  $w_c$  and  $\bar{d}$  are the values interpolated in  $w_c$  vs.  $t$  and  $\bar{d}$  vs.  $t$  curves at the corresponding times. Attrition rate constants  $k$  obtained by working out BFBC results according to this procedure are also given in Table 3.

The comparison between the various values of  $k$  shows the soundness of the BFBC technique in the characterization of the attrition behavior of the coal. In particular, the simple procedure based on data collected at  $t \geq t'$  and use of Eq. 17 gives  $k$  which

TABLE 3. EVALUATION OF THE ATTRITION RATE CONSTANTS OF THE COAL TESTED FROM RESULTS OF CFBC AND BFBC EXPERIMENTS

|                    | Feed Size,<br>mm  | Bed Sand<br>Size, mm | $U$ , cm s <sup>-1</sup> | $T$ , °C | Inlet | O <sub>2</sub> , % | $k \cdot 10^7$ from Eq. |      |      |      |
|--------------------|---|----------------------|--------------------------|----------|-------|--------------------|-------------------------|------|------|------|
|                    |   |                      |                          |          |       |                    | Outlet                  | 14   | 16   | 17   |
| Based on CFBC data |   |                      |                          |          |       |                    |                         |      |      |      |
| Coal               | 1-0.4; 3-1<br>6-3; 9-6  | 0.4-0.2              | 80-160                   | 650-950  | 21    |                    | 0.5-7                   | 1.86 | —    | —    |
|                    |   |                      | 80-160                   | 650-950  | 21    |                    | 0.5-1                   | 1.82 | —    | —    |
|                    |   |                      | 80-160                   | 750-950  | 21    |                    | 1-3                     | 2.05 | —    | —    |
|                    |   |                      | 80-160                   | 650-950  | 21    |                    | 3-7                     | 1.88 | —    | —    |
| Based on BFBC data |   |                      |                          |          |       |                    |                         |      |      |      |
| Char               | 6.35-4.76<br>6.35-4.76<br>6.35-4.76<br>6.35-4.76  | 0.4-0.3              | 80                       | 850      | 21    |                    | 16.8-21                 | —    | 1.44 | 1.84 |
|                    |   |                      | 80                       | 850      | 4.5   |                    | 3.6-4.5                 | —    | 1.33 | 2.02 |
|                    |   |                      | 80                       | 850      | 1.4   |                    | 1.1-1.4                 | —    | 1.28 | 1.17 |
|                    |   |                      | 80                       | 850      | 0     |                    | 0                       | —    | —    | 0.18 |
| Coal               | 4.76-4.00<br>6.35-4.76<br>6.35-4.76<br>6.35-4.76<br>6.35-4.76<br>6.35-4.76<br>6.35-4.76<br>6.35-4.76<br>6.35-4.76<br>6.35-4.76<br>6.35-4.76<br>6.35-4.76<br>9.00-6.35 | 0.4-0.3              | 80                       | 850      | 4.5   |                    | 3.2-4.5                 | —    | 1.99 | 1.82 |
|                    |   |                      | 50                       | 850      | 4.5   |                    | 3.6-4.5                 | —    | 1.38 | 1.30 |
|                    |   |                      | 80                       | 750      | 21    |                    | 17.3-21                 | —    | 3.25 | 3.52 |
|                    |   |                      | 80                       | 750      | 4.5   |                    | 3.5-4.5                 | —    | 2.77 | 2.41 |
|                    |   |                      | 80                       | 850      | 21    |                    | 16.7-21                 | —    | 1.90 | 1.81 |
|                    |   |                      | 80                       | 850      | 4.5   |                    | 3.5-4.5                 | —    | 2.30 | 2.07 |
|                    |   |                      | 80                       | 850      | 2.9   |                    | 2.2-2.9                 | —    | 2.69 | 2.14 |
|                    |   |                      | 80                       | 850      | 1.4   |                    | 1.1-1.4                 | —    | 0.76 | 1.02 |
|                    |   |                      | 80                       | 850      | 0.75  |                    | 0.58-0.75               | —    | 0.78 | 0.86 |
|                    |   |                      | 80                       | 850      | 0     |                    | 0                       | —    | —    | 0.13 |
|                    |   |                      | 80                       | 950      | 4.5   |                    | 3.3-4.5                 | —    | 1.09 | 0.86 |
|                    |   |                      | 110                      | 850      | 4.5   |                    | 3.3-4.5                 | —    | 2.10 | 2.26 |
|                    |   |                      | 80                       | 850      | 4.5   |                    | 3.7-4.5                 | —    | 2.60 | 2.28 |

are in reasonable agreement with the value  $1.86 \times 10^{-7}$  given for the same coal and bed solids by Arena et al. (1983) as an average from results of CFBC experiments. The confidence range with which this attrition rate constant was given includes the majority of the values of  $k$  from BFBC experiments. The deviations found for runs at bed temperatures of  $750^{\circ}\text{C}$  and  $950^{\circ}\text{C}$  and, to a lesser extent, at  $50$  and  $110 \text{ cm s}^{-1}$  might reflect side effects, not yet completely clarified, related to changes in the degree of post-combustion of fines detached from char particles or in the features of attrition themselves. Differences in the degree of postcombustion might also explain the moderate increase of  $k$  found with  $6.35\text{--}4.76 \text{ mm}$  coal, at  $850^{\circ}\text{C}$  and  $80 \text{ cm s}^{-1}$  as  $(\text{O}_2\%)_{\text{in}}$  is reduced from  $21$  to  $2.9$ . For further reduction from  $2.9$  to  $0.75$ ,  $k$  decreased from  $2.14 \times 10^{-7}$  to  $0.86 \times 10^{-7}$ , to become  $0.13 \times 10^{-7}$  when fluidizing with nitrogen. This tendency, which might be interpreted as the switching from combustion-assisted to purely mechanical attrition, does not immediately fit with  $k$  from CFBC data at different oxygen concentrations in exit gases. As shown in Table 3, these values of  $k$  are very close to the average  $1.86 \times 10^{-7}$  for all the  $(\text{O}_2\%)_{\text{out}}$ . Had the carbon been burnt inside the particulate phase and the gas been completely mixed in that phase, values of  $k$  from CFBC data at low  $(\text{O}_2\%)_{\text{out}}$  should have been comparable to those

from BFBC experiments at low inlet (and outlet)  $\text{O}_2\%$ . The discrepancy might depend on the fact that gas was not thoroughly mixed in the particulate phase and that a substantial fraction of carbon burned in the vicinity of the oxygen-rich gas bubbles in CFBC experiments. It should finally be noted that the reasonable agreement between  $k$  determined by working out BFBC data according to Eq. 16 or 17 reflects the limited generation of fines occurring during the fragmentation of the coal tested and the relatively short time required to activate the combustion-assisted attrition. For other coals using Eq. 16 might be more appropriate.

#### Application to Design

The characterization of the attrition behavior of the coal from BFBC experiments is conveniently made by evaluating the attrition rate constant  $k$ . Using Eqs. 7 and 13,  $k$  is converted into  $k'_a$  and  $k_a$ , both required in Eq. 10 for calculating the elutriation rate  $E_c$  of attrited carbon from a continuous combustor. The value of  $k'_a$  enters directly into this equation, while that of  $k_a$  enters indirectly through the attrition contribution (Eq. 6) to the overall char particle shrinkage rate  $(dd/dt)$ . This in turn enters in the population balance equation of char particles which determines  $P(d)$ .

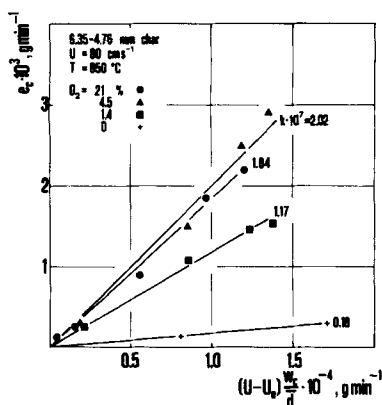


Figure 12. Evaluation of attrition rate constants based on Eq. 17 for char feed.

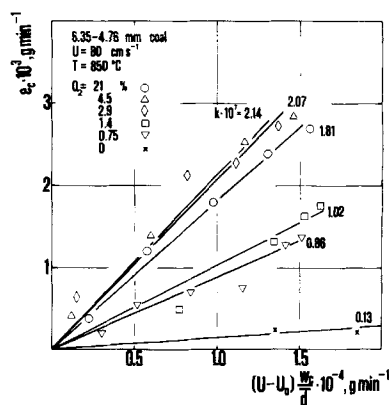


Figure 13. Evaluation of attrition rate constants based on Eq. 17 for coal feed.



In this connection, it should be noted that attrition contribution to  $(dd/dt)$  in Eq. 9 is small, being in general  $(dd/dt)_a/(dd/dt)$  less than 0.1. The error induced in  $P(d)$  can therefore be strongly affected by the uncertainties associated with the calculation of  $(dd/dt)_c$ , namely, by the degree of gas mixing to be assumed in the particulate phase or, in the case of complete mixing, by the oxygen concentration  $c_p$  in such a phase. As suggested by Eq. 10, uncertainties in  $P(d)$  directly propagate into  $E_c$  so that the occurrence of a poor contact between gas and solid inside the bed might result in elutriation rates of attrited carbon much higher than predicted even when a correct value of  $k$  is used. This fact should be taken into account when testing models for attrited carbon loss from fluidized bed combustors against results of operating units.

Finally, it should be borne in mind that values of  $k$  have been obtained from BFBC experiments intentionally designed to minimize postcombustion of carbon fines in the freeboard. Allowance for this effect must be made in model calculations of elutriation rates of attrited carbon from fluidized bed combustors where such conditions are not verified.

## ACKNOWLEDGMENT

The research was carried out within the framework of Progetto Finalizzato Energetica of C.N.R., Rome. The authors are indebted to A. Cammarota who helped in performing the experimental work. This paper was prepared with the support of the U.S. Department of Energy, Grant DE-FG22-81PC40796. However, any opinion, findings, conclusions, or recommendations expressed herein are those of the authors and do not necessarily reflect the views of DOE. Two of the authors (R.C. and A.M.) are grateful to Ansaldo S.p.A., Genova, for providing scholarships.

## NOTATION

|                  |   |
|------------------|---|
| $c_p$            | = oxygen concentration in the particulate phase of the fluidized bed  |
| $C$              | = mass fraction of carbon in the char   |
| $C_i$            | = initial mass fraction of carbon in the char   |
| $d, \bar{d}$     | = particle and surface-based average particle size of char in the bed   |
| $d_i, \bar{d}_i$ | = feed coal (or char) particle and initial surface-based average particle size of char in the bed                     |
| $d^*$            | = size of the shrunken char particle with terminal velocity equal to gas velocity at the freeboard outlet temperature |
| $D_g$            | = oxygen diffusivity  |
| $e_c$            | = instantaneous carbon elutriation (and attrition) rate in BFBC experiments   |
| $e_{ct}$         | = initial carbon elutriation rate   |
| $e_c$            | = relative maximum of the carbon attrition curve at $t > 0$   |
| $E_c$            | = carbon attrition rate in CFBC experiments   |
| $k, k_a, k'_a$   | = char attrition constants  |
| $k_s$            | = carbon reaction rate constant   |
| $M_c$            | = carbon atomic weight  |
| $N$              | = number of char particles in the bed   |
| $P(d)$           | = bed carbon particle size distribution on a numerical basis in CFBC experiments                                      |
| $P_w(d)$         | = bed carbon particle size distribution on a weight basis in CFBC experiments   |
| $Sh$             | = char particle Sherwood number   |
| $t$              | = time  |
| $t'$             | = time at which $e_c$ occurs  |
| $t_{bo}$         | = burnout time  |
| $T$              | = bed temperature   |
| $U$              | = fluidizing gas superficial velocity at bed temperature  |
| $U_o$            | = minimum fluidizing gas superficial velocity at bed temperature  |

|          |   |
|----------|---|
| $w_c$    | = bed carbon loading in BFBC experiments  |
| $w_{ct}$ | = initial bed carbon loading  |
| $w_c$    | = bed carbon loading at $t'$  |
| $W_c$    | = bed carbon loading in CFBC experiments  |
| $X_d$    | = mass fraction of char particles of size $d$                                     |
| $X_{dt}$ | = mass fraction of char particles of size $d$ at the end of coal devolatilization |

## Greek Letters

|          |   |
|----------|---|
| $\eta$   | = carbon combustion efficiency            |
| $\xi$    | = degree of conversion of injected carbon |
| $\rho_c$ | = carbon density of the char particle     |

## LITERATURE CITED

- Andrei, M., "Time-Resolved Burnout in the Combustion of Coal Particles in Fluidized Bed," M.S. Thesis in Chem. Eng., MIT, Cambridge, MA (1979).
- Arena, U., M. D'Amore, and L. Massimilla, "Carbon Attrition During the Fluidized Combustion of a Coal," *AIChE J.*, **29**, 40 (1983).
- Avedesian, M. M., and J. F. Davidson, "Combustion of Carbon Particles in a Fluidized Bed," *Trans. Inst. Chem. Engrs.*, **51**, 121 (1973).
- Beér, J. M., L. Massimilla, and A. F. Sarofim, "Fluidized Coal Combustion: the Effect of Coal Type on Carbon Load and Carbon Elutriation," Int. Conf. on Fluidised Combustion: Systems and Applications, *Inst. of Energy Symp. Ser.*, **4**, IV-5-1, London (1980).
- Borghi, G. G., A. F. Sarofim, and J. M. Beér, "A Model of Coal Devolatilization and Combustion in Fluidized Beds," *AIChE 70th Ann. Meet.*, New York (Nov., 1977).
- Chakraborty, R. K., and J. R. Howard, "Combustion of Single Carbon Particles in Fluidized Beds of High-Density Alumina," *J. Inst. of Energy*, **55**, (Mar. 1981).
- Chirone, R., et al., "Fragmentation and Attrition in the Fluidized Combustion of a Coal," Proc. 7th Int. Conf. on Fluidized Bed Combustion, U.S. Dept. of Energy, Washington DC, 1,023 (1982).
- D'Amore, M., G. Donsi, and L. Massimilla, "Bed Carbon Loading and Particle Size Distribution in Fluidized Combustion of Fuels of Various Reactivity," Proc. 6th Int. Conf. on Fluidized Bed Combustion, U.S. Dept. of Energy, Washington DC, 675 (1980).
- Donsi, G., et al., "The Calculation of Carbon Load and Axial Profiles of Oxygen Concentration in the Bed of a Fluidized Combustor," *Combustion Sci. & Tech.*, **21**, 25 (1979).
- Donsi, G., L. Massimilla, and M. Miccio, "Carbon Fines Production and Elutriation from the Bed of a Fluidized Coal Combustor," *Combustion and Flame*, **41**, 57 (1981).
- Jung, K., and R. D. La Nauze, "Sherwood Numbers for Burning Particles in Fluidized Beds," *Fluidization IV*, 4th Int. Conf. on Fluidization, Kashikojima, Japan (1983).
- Kunii, D., and O. Levenspiel, *Fluidization Engineering*, J. W. Wiley, New York (1969).
- La Nauze, R. D., and K. Jung, "The Kinetics of Combustion of Petroleum Coke Particles in a Fluidized-Bed Combustor," *Proc. of 19th Symp. (Int.) on Combustion*, 1,087, The Combustion Institute, Pittsburgh, PA (1982).
- Levenspiel, O., *Chemical Reaction Engineering*, J. W. Wiley, New York (1972).
- Massimilla, L., et al., "Carbon Attrition During the Fluidized Combustion and Gasification of Coal," DOE Quarterly Technical Report No. DOE/PC40796-7, U.S. Dept. of Energy, Washington DC (1983).
- Merrick, D., and J. Highley, "Particle Size Reduction and Elutriation in a Fluidized Bed Process," *AIChE Symp. Ser.*, No. 137, **70**, 366, (1974).
- Pillai, K. K., "The Influence of Coal Type on Devolatilization and Combustion in Fluidized Beds," *J. Inst. of Energy*, 142 (Sept., 1981).
- Ross, I. B., and J. F. Davidson, "The Combustion of Carbon Particles in a Fluidised Bed," *Trans. Inst. Chem. Engrs.*, **59**, 108 (1981).
- Vaux, W. G., "Attrition of Particles in the Bubbling Zone of a Fluidized Bed," *Proc. of the American Power Conference*, **40**, 793 (1978).
- Yates, J. G., and P. R. Walker, "Particle Temperatures in a Fluidized Bed Combustor," *Fluidization*, J. F. Davidson and D. L. Keairs, Cambridge Univ. Press (1978).

Manuscript received Nov. 4, 1983; revision received Mar. 14, 1984, and accepted Mar. 21.